14th International Conference on Structural Safety and Reliability - ICOSSAR'25
1-6 June, 2025 - Los Angeles California, USA
R. Ghanem, E. Johnson, S. Masri and A. Olivier (Eds)

PHYSICS-INFORMED POLYNOMIAL CHAOS EXPANSIONS FOR GEOMETRIC UNCERTAINTIES

NATALY A. MANQUE[1,*], MARCOS A. VALDEBENITO[1], LUKÁŠ NOVÁK[2], MATTHIAS G.R. FAES[1,3]

[1] Chair for Reliability Engineering, TU Dortmund University,
Leonhard-Euler-Str. 5, Dortmund 44227, Germany
{nataly.manque, marcos.valdebenito, matthias.faes}@tu-dortmund.de

[2] Department of Civil Engineering, Brno University of Technology, Brno, Czech Republic,
Veveří 331/95 602 00 Brno, Czech Republic
lukas.novak4@vut.cz

[3] International Joint Research Center for Engineering Reliability and Stochastic Mechanics,
Tongji University, Shanghai 200092, China
matthias.faes@tu-dortmund.de

Key words: Polynomial Chaos Expansion (PCE), Isogeometric Analysis (IGA), Geometric Uncertainty, Variational Sensitivity Analysis, Physical Constraints, Surrogate Model.

Abstract. Collecting large experimental datasets that accurately depict the behavior of complex systems under uncertainty poses a significant challenge. In such scenarios, surrogate models such as Polynomial Chaos Expansion (PCE) benefit from incorporating problem-specific physical information. This integration facilitates the reduction of the necessary training data, thereby enabling efficient estimation of the system's response. Nevertheless, when uncertainties arise from geometric variations, traditional Finite Element Analysis (FEA) methods are limited in generating training datasets for PCE coefficient estimation due to mesh dependency and potential inaccuracies in geometry approximation. To address these limitations, this study explores a novel methodology that uses Isogeometric Analysis (IGA) to generate physical insights for systems with geometric uncertainties. These insights are then employed to construct a Physics-informed PCE (PC^2), which directly integrates IGA sensitivities to embed constraints, such as boundary conditions and system behavior, into the surrogate model. The corresponding sensitivities are computed as a by-product of the analysis using a variational approach. A case study demonstrates the efficacy of the method in predicting complex responses, such as stress triaxiality, while maintaining a balance between computational cost and accuracy. Furthermore, the results demonstrate a 40% reduction in mean squared error (MSE) when employing the proposed IGA-sensitivity-based PC^2 in contrast to sparse Least Angle Regression (LAR) PCE. This suggests that the proposed strategy can provide more accurate estimates than traditional PCE approaches applied to geometric uncertainties, highlighting its potential for broader uncertainty quantification and surrogate modeling applications.

1 INTRODUCTION

Geometric uncertainties are prevalent in diverse fields, from aerospace to biomedical engineering, where precision and robustness are of the utmost importance. The increasing complexity of modern systems in these domains demands more accurate modeling of such uncertainties. Appropriate treatment of this uncertainty is critical to determining key factors, from boundary conditions to displacement and stress fields. Slight variations in thickness, length, curvature, or shape can significantly affect performance, leading to stress concentrations or changes in natural frequencies [1]. Yet geometry is typically approximated when using numerical models such as Finite Element Analysis (FEA) [2]. Moreover, complex shapes and non-smooth geometries typically require a large number of degrees-of-freedom for their construction. Consequently, direct propagation of geometric uncertainty through a high-dimensional parameter space becomes impractical.

Isogeometric Analysis (IGA) [3] addresses these challenges by unifying design and analysis. IGA employs exact Computer-Aided Design (CAD) geometries, described by Non-Uniform Rational B-Splines (NURBS), directly in the solver, avoiding geometric approximation. The primary advantage of IGA for uncertainty quantification (UQ) lies in controlling geometry via NURBS control points, whose variation bypasses the cost of FEA re-meshing when exploring geometric variations.

Surrogate modeling techniques like Polynomial Chaos Expansion (PCE) [4] further reduce cost by expressing the stochastic response as an orthogonal polynomial series with coefficients computed via regression. Sparse techniques such as least-angle regression (LAR) [5] make PCE robust even with limited or noisy data. Recently, Physics-informed PCE (PC^2) [6] extended this framework by embedding physical constraints directly into the coefficient estimation. A Lagrange-multiplier formulation yields a Karush–Kuhn–Tucker system that enforces both data fidelity and governing equations, yielding accurate surrogates from few model evaluations.

Early PCE treatments of geometric uncertainty relied on mesh-node parametrization with FEA re-meshing [7]. Subsequent stochastic-domain approaches improved efficiency through fictitious domains [8] and mapping techniques [9], while Stochastic Isogeometric Analysis (SIGA) [10] leveraged NURBS basis functions for shape uncertainty. Recent Poincaré chaos expansions [11] advanced derivative-based sensitivity analysis through orthonormal eigenfunctions, yet focused on Sobol' index estimation rather than physics-constrained function approximation. Crucially, none integrate IGA's exact geometry and variational sensitivities with physics-informed PCE. To the best of authors knowledge, this study is the first to integrate IGA-derived variational sensitivities directly into the PC^2 framework for geometric UQ.

Accordingly, this paper use IGA to compute variational sensitivities for linear-elastic systems with independent random geometric parameters. These insights form the KKT constraints in a physics-informed PCE trained via Latin Hypercube Sampling (LHS). The proposed IGA-sensitivity-based PC^2 strategy is tested for estimating the stress triaxiality response of a 3D linear system with four uncertain geometric parameters. The results demonstrate that the IGA-sensitivity-based PC^2 surrogate outperforms standard sparse PCE applied to geometric uncertainties in both accuracy and efficiency.

2 PHYSICS-INFORMED POLYNOMIAL CHAOS EXPANSIONS

2.1 Formulation of the problem

Consider a linear system subjected to static loads, where the parameters defining the system's geometry (such as lengths, thicknesses, and curvatures) are uncertain. These uncertainties may arise from the variability in manufacturing processes, fluctuations in environmental conditions, or

long-term service effects. Therefore, it is assumed that the uncertainty affecting the system exhibits an aleatory nature. These uncertain geometric parameters are modeled by a set of independent random variables $\boldsymbol{\mathcal{X}} = (\mathcal{X}_1, \mathcal{X}_2, \ldots, \mathcal{X}_M)$, with M the number of uncertain parameters, with known probability density functions (PDFs) $f_{\mathcal{X}_i}(x_i)$, $i = 1, \ldots M$. A realization of $\boldsymbol{\mathcal{X}}$ is denoted by $\boldsymbol{x} = (x_1, x_2, \ldots, x_M)$. To evaluate the structural behavior of this system, a set of partial differential equations (PDEs) governing the physics must be solved. To obtain an approximate solution to these PDEs through a numerical model $\mathcal{M}(\boldsymbol{x})$, the Finite Element Method (FEM) [2], Isogeometric Analysis (IGA) [3], or any of its variations can be applied. Note that the model $\mathcal{M}(\boldsymbol{x})$ depends on the realizations of the geometric uncertain parameters $\boldsymbol{x}$. The output of the model, denoted by $\boldsymbol{y}$, represents the system's response (such as displacements, stresses, or strains) and is defined as the mapping,

$$\mathcal{M}(\boldsymbol{x}) : \boldsymbol{y} = m(\boldsymbol{x}) \tag{1}$$

where m is a response function operator that maps realizations of the geometric uncertain input parameters $\boldsymbol{x}$ to the output response $\boldsymbol{y}$. It is important to note that the behavior of the system is influenced by the randomness of the input vector $\boldsymbol{\mathcal{X}}$ during the mapping with m. Consequently, the response of the system is subject to uncertainties as well. Therefore, for the case of scalar outputs, the uncertainty of the system's output y is represented by a random variable $\mathcal{Y}$.

Solving the numerical model $\mathcal{M}(\boldsymbol{x})$ of Eq. (1) for different realizations of the uncertain geometric parameters $\boldsymbol{x}$ can be computationally expensive, particularly when using high-fidelity simulations such as FEM or IGA. Surrogate modeling techniques like Polynomial Chaos Expansion (PCE) [4] provide an effective alternative to efficiently quantify this uncertainty. In the next subsection, the approximate representation of the model $\mathcal{M}(\boldsymbol{x})$ response is studied using PCE.

2.2 Polynomial Chaos Expansion

Polynomial Chaos Expansion (PCE) [4] provides a well-established framework for approximating the response of complex systems by representing the output as a series of orthogonal polynomial basis functions. This approach significantly reduces the computational cost compared to Monte Carlo simulations, under certain circumstances. In the case that the stochastic response of the system is scalar, that is $\mathcal{Y}$, under the assumption that it has a finite variance, and if the Doob-Dynkin lemma is satisfied (ensuring measurability of the response with respect to $\boldsymbol{\mathcal{X}}$), $\mathcal{Y}(\boldsymbol{\mathcal{X}})$ is expressed as,

$$\mathcal{Y}(\boldsymbol{\mathcal{X}}) = \sum_{\boldsymbol{\alpha} \in \mathbb{N}^M} y_{\boldsymbol{\alpha}} \Psi_{\boldsymbol{\alpha}}(\boldsymbol{\mathcal{X}}), \tag{2}$$

where $\boldsymbol{\alpha}$ is a multi-index that defines the polynomial degree in each variable, $y_{\boldsymbol{\alpha}} \in \mathbb{R}$ represents the expansion coefficient (which needs to be determined) of the polynomial basis function associated with the multi-index $\boldsymbol{\alpha}$, and $\Psi_{\boldsymbol{\alpha}}(\boldsymbol{\mathcal{X}})$ are multivariate orthogonal polynomials.

Since it is assumed that $\boldsymbol{\mathcal{X}}$ contains independent random variables, the multivariate polynomial functions are constructed as tensor products of univariate polynomials orthonormal with respect to the marginal PDFs of each $\mathcal{X}_i$. In mathematical terms, the multivariate basis functions are defined as,

$$\Psi_{\boldsymbol{\alpha}}(\boldsymbol{\mathcal{X}}) = \prod_{i=1}^{M} \phi_{\alpha_i}^{(i)}(\mathcal{X}_i), \tag{3}$$

where $\phi_{\alpha_i}^{(i)}(\mathcal{X}_i)$ are orthonormal polynomials in the $i-$th parameter of degree α_i satisfying,

$$\langle \phi_{\alpha_i}^{(i)}, \phi_{\beta_i}^{(i)} \rangle = \int_{\mathcal{D}_{\mathcal{X}_i}} \phi_{\alpha_i}^{(i)}(x_i) \phi_{\beta_i}^{(i)}(x_i) f_{\mathcal{X}_i}(x_i) dx_i = \delta_{\alpha_i \beta_i}. \tag{4}$$

Here $\mathcal{D}_{\mathcal{X}_i}$ is the domain of the random variable $\mathcal{X}_i$, and $f_{\mathcal{X}_i}(x_i)$ represents the probability density function (PDF) of the random variable $\mathcal{X}_i$, where x_i denotes a realization of $\mathcal{X}_i$. $\delta_{\alpha_i \beta_i}$ is the Kronecker delta, which equals 1 if $\alpha_i = \beta_i$ and 0 otherwise, ensuring orthogonality of the basis functions.

To make the expansion computationally feasible, it is truncated to a finite number of terms P as,

$$\mathcal{Y}^{\text{PCE}}(\boldsymbol{\mathcal{X}}) = \sum_{\boldsymbol{\alpha} \in \mathcal{A}} y_{\boldsymbol{\alpha}} \Psi_{\boldsymbol{\alpha}}(\boldsymbol{\mathcal{X}}). \tag{5}$$

where the truncation set $\mathcal{A}$ follows,

$$\mathcal{A}_{M,p_p} = \{\boldsymbol{\alpha} \in \mathbb{N}^M : \|\boldsymbol{\alpha}\|_1 \leq p_p\}. \tag{6}$$

Here $\mathcal{Y}^{\text{PCE}}(\boldsymbol{\mathcal{X}})$ is the truncated PCE approximation of the system's response, and $\mathcal{A}_{M,p_p}$ is the truncation set that defines which polynomial terms are included in the expansion. Moreover, p_p is the maximum polynomial degree in the expansion, and $\|\cdot\|_1$ denotes the L^1 norm. Note that due to this truncation, only terms whose total degree $\|\boldsymbol{\alpha}\|_1$ is less than or equal to a predefined p_p are retained; however, in practice, one can choose any truncation rule.

The number of terms in the truncated expansion P is given by,

$$P = \frac{(M + p_p)!}{M! p_p!}. \tag{7}$$

Notably, the truncated expansion introduces an error ϵ, that is,

$$\mathcal{Y} = \mathcal{Y}^{\text{PCE}} + \epsilon = \sum_{\boldsymbol{\alpha} \in \mathcal{A}} y_{\boldsymbol{\alpha}} \Psi_{\boldsymbol{\alpha}}(\boldsymbol{\mathcal{X}}) + \epsilon. \tag{8}$$

From Eq. (8), the coefficients $\boldsymbol{y}_{\boldsymbol{\alpha}}$ are determined by minimizing the discrepancy between the PCE surrogate $\mathcal{Y}^{\text{PCE}}(\boldsymbol{\mathcal{X}})$ and true model evaluations from an experimental design (ED) $\{\boldsymbol{x}^{(i)}, y^{(i)}\}_{i=1}^{n_{\text{sim}}}$, where $y^{(i)} = \mathcal{M}(\boldsymbol{x}^{(i)})$ are realizations of $\mathcal{Y}$. This is because, from a statistical perspective, the truncated PCE in Eq. (5) can be considered a linear regression model with an intercept. Then the coefficients $\boldsymbol{y}_{\boldsymbol{\alpha}}$ can be determined using ordinary least squares (OLS), that is,

$$\boldsymbol{y}_{\boldsymbol{\alpha}} = (\boldsymbol{\Psi}^{\mathsf{T}} \boldsymbol{\Psi})^{-1} \boldsymbol{\Psi}^{\mathsf{T}} \boldsymbol{y}^{\boldsymbol{D}} \tag{9}$$

where $\boldsymbol{\Psi}$ is the data (or regression) matrix, i.e. the PCE basis evaluations at the training points from the ED $\{\boldsymbol{x}^{(i)}, y^{(i)}\}_{i=1}^{n_{\text{sim}}}$, and $\boldsymbol{y}^D = [y^{(1)}, \ldots, y^{(n_{\text{sim}})}]^{\mathsf{T}}$ is the model evaluations vector. Once the coefficients $\boldsymbol{y}_{\boldsymbol{\alpha}}$ are found, it is possible to estimate statistical moments of the output from the expansion directly. This makes uncertainty quantification (UQ) tasks straightforward [12]. As can be observed in Eq. (7), since the number of terms P grows with the input dimension M and the maximum polynomial degree in the expansion p_p, OLS typically requires samples on the order of $\mathcal{O}(P \ln(P))$ for a well-posed fit, which can be prohibitive for large M and p_p, especially for complex systems. To alleviate this, one can apply sparse regression methods, such as Least Angle Regression (LAR) [5],

to identify a smaller, optimally informative subset of basis functions, thereby reducing both computational and sampling effort. While powerful, this conventional PCE framework often requires a large ED to achieve accuracy in high-dimensional problems. To address this issue, the Physics-informed Polynomial Chaos Expansion (PC^2) has recently been introduced [6], which incorporates known physical laws (e.g., governing PDEs, boundary conditions) as constraints during the surrogate construction [13]. This approach reduces the need for costly model evaluation while ensuring the surrogate adheres to the underlying physics. The details for its implementation are described in the next subsection.

2.3 Physics-informed Polynomial Chaos Expansions

Building on the PCE framework from Section 2.2, Physics-Informed Polynomial Chaos Expansion (PC^2) [6] incorporates physical constraints derived from the governing PDEs of Eq. (1) and associated boundary conditions. Consider that the system's response satisfies,

$$\mathcal{L}(\boldsymbol{x}, \mathcal{Y}^{\text{PCE}}(\boldsymbol{x})) = f(\boldsymbol{x}), \quad \boldsymbol{x} \in \mathcal{D}, \tag{10}$$

with boundary conditions $\mathcal{B}(\boldsymbol{x}, \mathcal{Y}^{\text{PCE}}(\boldsymbol{x})) = g(\boldsymbol{x})$ for $\boldsymbol{x} \in \partial\mathcal{D}$, where $\mathcal{L}$ and $\mathcal{B}$ are differential operators, and f, g are source terms.

The PC^2 coefficients $\boldsymbol{y}_{\boldsymbol{\alpha}}$ are found by solving a constrained extension of the OLS problem in Eq. (9), that is,

$$\min_{\boldsymbol{y}_{\boldsymbol{\alpha}}} \|\boldsymbol{y}^D - \boldsymbol{\Psi}\boldsymbol{y}_{\boldsymbol{\alpha}}\|^2 \quad \text{subject to} \quad \boldsymbol{A}\boldsymbol{y}_{\boldsymbol{\alpha}} = \boldsymbol{c}, \tag{11}$$

where $\boldsymbol{A}$ encompasses the PDE and BC constrains, and $\boldsymbol{c}$ contains boundary values. Note that constructing the $\boldsymbol{A}$ matrix requires derivatives of the PCE model. This is because the matrix $\boldsymbol{A}$ enforces physics by evaluating the boundary operator $\mathcal{B}$ and PDE operator $\mathcal{L}$ on the PCE basis functions $\boldsymbol{\Psi}$. The corresponding derivatives are computed analytically using the polynomial properties. For details, the reader is referred to [6].

The solution of Eq. (11) is obtained via the Karush-Kuhn-Tucker (KKT) conditions,

$$\begin{bmatrix} \boldsymbol{\Psi}^{\mathsf{T}}\boldsymbol{\Psi} & \boldsymbol{A}^{\mathsf{T}} \\ \boldsymbol{A} & \boldsymbol{0} \end{bmatrix} \begin{bmatrix} \boldsymbol{y}_{\boldsymbol{\alpha}} \\ \boldsymbol{\lambda} \end{bmatrix} = \begin{bmatrix} \boldsymbol{\Psi}^{\mathsf{T}}\boldsymbol{y}^D \\ \boldsymbol{c} \end{bmatrix}, \tag{12}$$

where $\boldsymbol{\lambda}$ are Lagrange multipliers. This ensures that the experimental data and the laws of physics are both satisfied while minimizing the square error of the PCE expansion. To solve Eq. (12) the PC^2 framework employs three discrete sets of samples, namely: experimental design, boundary points and virtual points. Each of these set of samples is described in the following. The experimental design (ED) $\{\boldsymbol{x}^{(i)}, y^{(i)}\}_{i=1}^{n_{\text{sim}}}$ is obtained from the direct evaluation of the PDE from Eq. (1) within the domain $\mathcal{D}$. These evaluations populate the regression matrix $\boldsymbol{\Psi}$ of Eq. (9) and link the surrogate to the responses of the underlying true model. Boundary points, $\{\boldsymbol{x}^{(b)}\}_{b=1}^{n_{\text{BC}}}$ prescribed locations on $\partial\mathcal{D}$, where Dirichlet/Neumann boundary conditions $\mathcal{B}(\mathcal{Y}^{\text{PCE}}) = g(\boldsymbol{x}^{(b)})$ are enforced. These ensure geometric compliance with the constraints of the problem. Finally, virtual points $\{\boldsymbol{x}^{(v)}\}_{v=1}^{n_{\text{V}}}$ correspond to artificial collocation points in $\mathcal{D}$, where the PDE residual $\mathcal{L}(\mathcal{Y}^{\text{PCE}}) = f(\boldsymbol{x}^{(v)})$ is minimized. These inject physical consistency without requiring model evaluations. The last two groups of points, n_{BC} and n_{V}, populate the constraint matrix $\boldsymbol{A}$ in the KKT system of Eq. (12).

These sets are mutually independent, and their sizes (n_{sim}, n_{BC}, n_{V}) can be assigned arbitrarily, provided that it is ensured that,

$$P \leq n_{\text{sim}} + n_{\text{BC}} + n_{\text{V}}, \tag{13}$$

where P is the number of PCE terms from Eq. (7). In this paper, the calculations related to the PC^2 model were done using UQPy [14]. The strategy used to construct the discrete dataset required to build the PC^2 model is defined in Section 4.

3 ISOGEOMETRIC ANALYSIS

As mentioned in the previous section, this paper investigates applying sensitivities derived from the Isogeometric Analysis (IGA) model to integrate physical insights into Polynomial Chaos Expansion (PCE). This section aims to succinctly explain the fundamentals of IGA and illustrate why this method is suitable for exploring geometric variations and, consequently, generating the necessary dataset to train the Physics-informed Polynomial Chaos Expansions (PC^2) using IGA sensitivities.

3.1 NURBS basis functions

Isogeometric Analysis (IGA) can be regarded as a classic Finite Element Analysis (FEA) generalization. The most important feature of this method is the underlying basis functions, which originate from the Computer-Aided Design (CAD) field [15]. In FEA, geometry is approximated using polynomial shape functions, whereas IGA employs B-Splines-based shape functions for a smoother geometric representation and solution approximation. In most cases, Non-Uniform Rational B-Splines (NURBS) are utilized as basis functions. These smooth geometric descriptions are defined in the parametric space $\tilde{\Omega}$ using control points and knot vectors $\boldsymbol{\Xi}$, given by

$$\boldsymbol{\Xi} = \left\{\xi_1, \xi_2, \ldots, \xi_{n+p+1}\right\}, \tag{14}$$

where ξ_i define the knots, p corresponds to the NURBS order, C^{p-1-k} is the continuity conditions at the knots, k denotes the number of repetitions of a specific knot in the knot vector $\boldsymbol{\Xi}$, and n is the total number of basis functions. Note that the knot vectors must have $n + p + 1$ increasing entries.

For one-dimensional descriptions, NURBS basis functions correspond to

$$R_{i,p}(\xi) = \frac{w_i N_{i,p}(\xi)}{W(\xi)}, \quad 1 \leq i \leq p+1, \quad \text{with} \quad W(\xi) = \sum_{i=1}^{\mathsf{n_{cp}}} w_i N_{i,p}(\xi), \tag{15}$$

where $\mathsf{n_{cp}}$ is the total number of NURBS control points, $w_i > 0$ are weight factors, and $N_{i,p}$ are B-spline basis functions of order p [16]. By definition, NURBS are only interpolatory at the ends of the parameter interval spanned by their corresponding knot vectors, but, in general, not at interior knots. These continuity properties make NURBS excellent candidates for basis functions for FEA formulations. NURBS curves $\mathbf{C}(\xi, \boldsymbol{x})$, surfaces $\mathbf{S}(\xi, \eta, \boldsymbol{x})$ and volumes $\mathbf{V}(\xi, \eta, \zeta, \boldsymbol{x})$ are respectively described by,

$$\begin{aligned} \mathbf{C}(\xi, \boldsymbol{x}) &= \sum_{i=1}^{n} R_{i,p}(\xi)\mathbf{P}_i(\boldsymbol{x}), \quad \mathbf{S}(\xi, \eta, \boldsymbol{x}) = \sum_{i=1}^{n}\sum_{j=1}^{m} R_{i,p}(\xi)R_{j,q}(\eta)\mathbf{P}_{i,j}(\boldsymbol{x}), \\ \mathbf{V}(\xi, \eta, \zeta, \boldsymbol{x}) &= \sum_{i=1}^{n}\sum_{j=1}^{m}\sum_{k=1}^{l} R_{i,p}(\xi)R_{j,q}(\eta)R_{k,r}(\zeta)\mathbf{P}_{i,j,k}(\boldsymbol{x}), \end{aligned} \tag{16}$$

where $\boldsymbol{x}$ represents uncertain geometric parameters (e.g., lengths, thicknesses, radii), $\mathbf{P}(\boldsymbol{x})$ contains control point coordinates, and $R_{i,p}(\xi)$, $R_{j,q}(\eta)$, $R_{k,r}(\zeta)$ are NURBS basis functions of degrees p, q,

r in the ξ-, η-, and ζ-directions. Here, n, m, and l denote the number of basis functions in each parametric direction, while ξ, η, and ζ correspond to parametric coordinates defined by knot vectors $\boldsymbol{\Xi}$, $\mathbf{H}$, and $\mathbf{Z}$ (see Eq. (14)). This description of the geometry renders the integration of uncertainty practical. Specifically, changes in the control point positions will result in the generation of new geometries.

Following the finite element formulation, the key point to define the IGA formulation is to resort to the weak equilibrium equation. The discretized matrix form of the weak equilibrium equation differs from the FEA formulation only in the choice of shape functions, which correspond to the NURBS defined in Eq. (15). For a detailed explanation of the procedure, the reader is referred to (Hughes et al., 2005) [3]. It is noteworthy that, unlike FEA, in IGA the response in terms of displacements is given at the positions of the control points. With the solution of the IGA model for the displacement, any response function of interest can be computed within a post-processing step similar to FEA. Once the solution of the IGA model is obtained, its sensitivities with respect to the uncertain geometric parameters can be determined using Variational Sensitivity Analysis [17]. The information in this sensitivity can be considered to train the PC^2 model. The described isogeometric model has been implemented in `MatLab` utilizing the NURBS toolbox, cf. [18]. The next subsection defines this sensitivity analysis for a general response of interest (e.g., displacements, stresses, or strain fields).

3.2 Variational sensitivity analysis

The generation of data for the training of the PC^2 is achieved by leveraging sensitivities from the IGA model to impose the physics. Given the advantage of IGA to explore geometry modifications, one can perform Variational Sensitivity Analysis [17]. The sensitivity analysis facilitates the evaluation of how variations in uncertain geometric parameters (such as lengths, thicknesses and radii), represented by $\boldsymbol{x}$, affect the response functions, denoted by $f(\boldsymbol{y}(\boldsymbol{x}), \boldsymbol{x})$. As outlined in [17], this approach leads to the expression

$$\delta f = \delta_y f + \delta_x f = \left[\frac{\partial f}{\partial \boldsymbol{y}}\right] \delta \boldsymbol{y} + \left[\frac{\partial f}{\partial \boldsymbol{x}}\right] \delta \boldsymbol{x}, \tag{17}$$

where $\delta_y f$ represents the contribution to the sensitivity from changes in the system's response, and $\delta_x f$ represents the contribution from variations in the geometry. The derivation of these sensitivities employs the direct differentiation method (DDM), wherein the equilibrium condition is maintained for any variation in the design geometry, $\delta \boldsymbol{x}$.

In certain applications, it is beneficial to parameterize the design geometry using specific geometric variables $\boldsymbol{x}$, such as thickness, lengths, or radii. In other words, the IGA control point matrix $\mathbf{P}$ is represented parametrically. This parametrization introduces the design-velocity matrix $\mathbf{D}(\boldsymbol{x})$, allowing the control points to be expressed as

$$\delta \mathbf{P}(\boldsymbol{x}) = \mathbf{D}(\boldsymbol{x})\, \delta \boldsymbol{x}. \tag{18}$$

This projection ensures that the sensitivity analysis explicitly accounts for changes in the uncertain parameters, enabling a deeper understanding of their impact on system responses while reducing computational cost. Once the sensitivities from the IGA model have been computed, they can be used to incorporate the physical constraints derived from the governing PDEs when developing the PC^2 model.

4 PROPOSED STRATEGY

4.1 IGA-sensitivity-based Physics-informed Polynomial Chaos Expansions

To integrate the IGA-derived sensitivity information the goal is to solve the constrained least squares problem of Eq. (11), but enforce agreement between PCE derivatives and IGA-derived sensitivities at n_{S} specified sensitivity points. In mathematical terms,

$$\min_{\boldsymbol{y}_{\boldsymbol{\alpha}}} \|\boldsymbol{y}^{D} - \boldsymbol{\Psi}\boldsymbol{y}_{\boldsymbol{\alpha}}\|^{2} \quad \text{subject to} \quad \boldsymbol{J}\boldsymbol{y}_{\boldsymbol{\alpha}} = \boldsymbol{s}, \tag{19}$$

where $\boldsymbol{J}$ is the Jacobian matrix of PCE basis derivatives at sensitivity points n_{S}, and $\boldsymbol{s}$ are the IGA-derived sensitivity values obtained from the variational sensitivity analysis.

The integrated framework is illustrated in Figure 1, for an arbitrary response surface and considering, for simplicity, the sensitivity information with respect to one uncertain parameter. The IGA solver discretizes the physical domain Ω using NURBS basis functions (see Eq. (15)) defined on the parametric domain $\tilde{\Omega}$, where control points $\mathbf{P}(\boldsymbol{x})$ form the control mesh. Key transitions of an element Ω_e from physical, to parametric $\tilde{\Omega}$, and further parent domain (highlighted by red arrows) exemplify the exact geometric representation and numerical efficiency of using IGA. The PDE solution, computed at knot positions, is mapped back to the physical space, where the system's response can be obtained through FEA postprocessing.

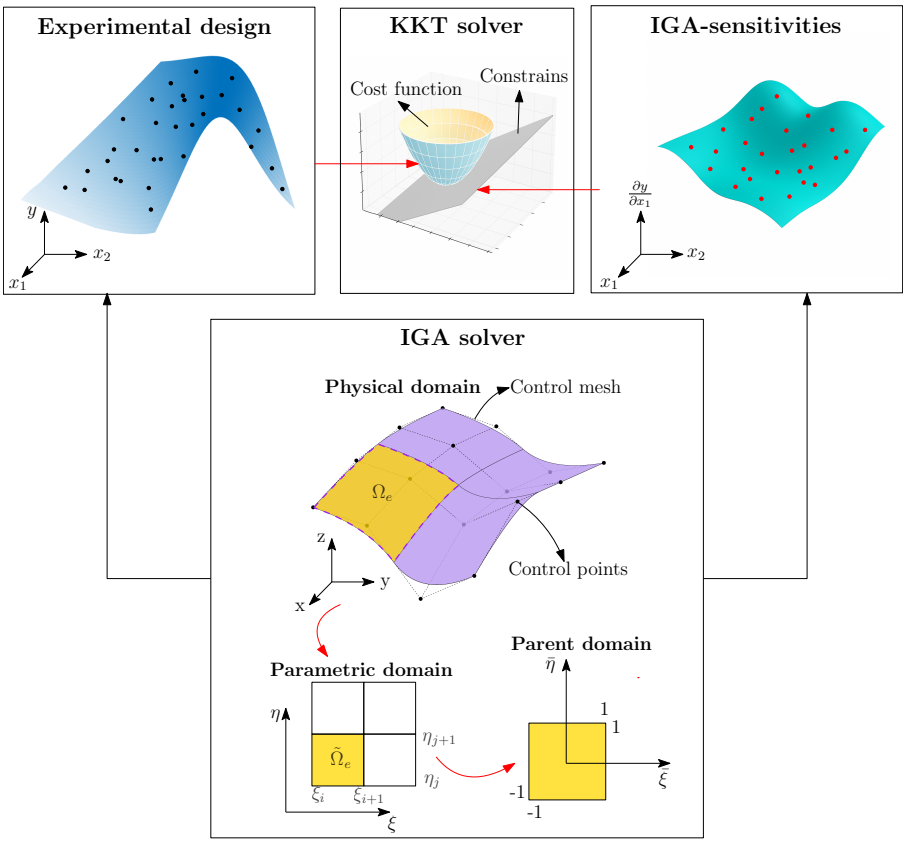

Figure 1: Scheme of the proposed IGA-sensitivity-based Physics-informed PCE.

Latin Hypercube Sampling (LHS) generates the experimental design ED (in black) over the response surface by evaluating the IGA model, while variational sensitivity analysis simultaneously computes geometric derivatives at n_{S} (in red) collocation points using the design-velocity matrix $\mathbf{D}(\boldsymbol{x})$ (Eq. (18)). Leveraging both the ED (n_{sim} samples) and IGA-derived sensitivities (n_{S} constraints), the KKT solver is applied (Eq. (19)), thereby enforcing physical consistency between the PCE surrogate and IGA model through explicit derivative matching. Furthermore, just as PC^2 benefits from using sparse solvers, the proposed approach can be coupled with least-angle regression (LAR).

5 EXAMPLE

5.1 Solid horseshoe

The proposed method is used to calculate the maximum stress triaxiality of a three-dimensional horseshoe-shaped solid, adapted from Hughes (2005) [3]. The horseshoe is subjected to equal and opposite in-plane flat-edge unit-magnitude displacements (see Figure 2). The base ends of the horseshoe are fixed in the $y-$direction, while only the outer corners are fixed in the $z-$direction. In the $x-$direction, a deterministic prescribed unit-magnitude displacement of $-u_0$ is applied to the left side, while a deterministic prescribed unit-magnitude displacement of u_0 is applied to the right side. Further, the displacements in the $x-$direction are restricted at the center of the top of the horseshoe.

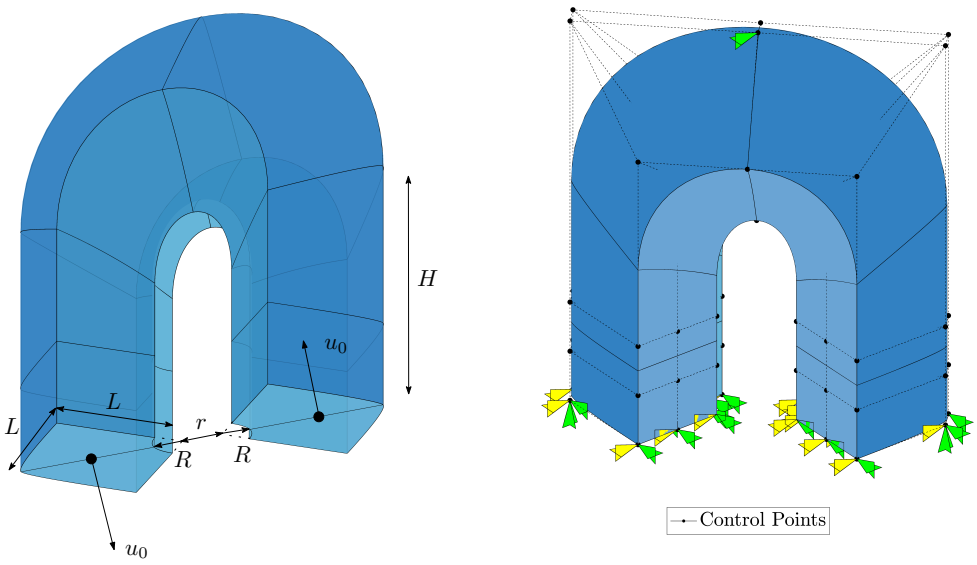

Figure 2: Uncertain geometric parameters of solid horseshoe 3D model for stress triaxiality analysis and prescribed displacements (left). Isogeometric model and boundary conditions (right).

The material properties of the horseshoe system are assumed to be deterministic and equal to $E = 3 \times 10^7\,\mathrm{N/cm^2}$ for Young's modulus and $\nu = 0.3$ for Poisson's ratio. The horseshoe geometry is constructed by performing a U-sweep on a square cross-section of dimensions $L \times L$, from which a quarter disk of radius R is subtracted to define the inner edge. The outer edge has a slightly rounded end which is defined by the value of L. Moreover, the horseshoe definition includes a straight portion of height H, and the distance between the origin and the center of the quarter disk is defined by r (see Figure 2). The NURBS volume used to represent the horseshoe-shaped geometry is based on $\mathsf{n}_{\mathsf{cp}} = 108$ control points, which comprises 324 degree-of-freedom. A parametric representation of the coordinates of each control point in terms of L, R, r, and H is proposed to translate the uncertainty in

the geometric input parameters into the NURBS control point matrix. A full definition of the NURBS model can be found in [19].

The geometric parameters are modeled as independent uniform random variables: $L \sim \mathcal{U}(3.5, 5.5)$, $R \sim \mathcal{U}(0.5, 1.5)$, $r \sim \mathcal{U}(0.9142, 1.9142)$, and $H \sim \mathcal{U}(7.5, 8.5)$, with all values in cm. These bounds reflect manufacturing tolerances and service-induced variability described in Section 2.1. The experimental design (ED) is generated by Latin Hypercube Sampling (LHS). Here, a total of 1000 realizations of the complete random input vector were computed using the IGA model. For each realization, the sensitivities of maximum stress triaxiality with respect to the geometric parameters were evaluated. Then, the sensitivity data were used to estimate the PCE coefficients in order to incorporate the governing physics into the surrogate construction. The results were calculated for multiple runs of n_{sim}.

The performance of PC^2 (in red), PC^2 LAR (in green), and standard LAR PCE (in blue) is compared in Fig. 3 using three error metrics: standard mean squared error (MSE), cumulative absolute error, and derivative MSE, plotted against the number of high-fidelity training runs n_{sim}. In the figure, the PC^2 and PC^2 LAR results are computed here using the proposed IGA sensitivity-based PC^2 method. The results are presented with convergence plots showing the mean $\pm\sigma$ intervals, for all error metrics. At the smallest experimental design ($n_{\mathrm{sim}} = 200$), the sparse physics-informed surrogate PC^2 LAR already matches the MSE of standard LAR PCE, demonstrating that enforcing physics does not compromise accuracy when data are scarce. As n_{sim} grows to 1000, full PC^2 achieves roughly a 40% reduction in MSE compared to LAR PCE, accompanied by substantial reductions in cumulative absolute error and improvements in gradient fidelity. Beyond $n_{\mathrm{sim}} \approx 600$, the error curves for PC^2 plateau, indicating that the surrogate has fully assimilated the equilibrium and boundary constraints and requires minimal additional simulations to reach its optimal accuracy. In terms of cumulative absolute error, PC^2 and PC^2 LAR again outperformed standard LAR PCE, with the smallest cumulative error over all samples. Furthermore, PC^2 and PC^2 LAR accuracy in derivative errors reflect their ability to preserve equilibrium laws (via IGA sensitivities), ensuring gradients align with physical behavior. Overall, both PC^2 variants consistently outperform standard sparse PCE, highlighting their robustness to extreme geometric variations due to the integration of IGA-derived sensitivities.

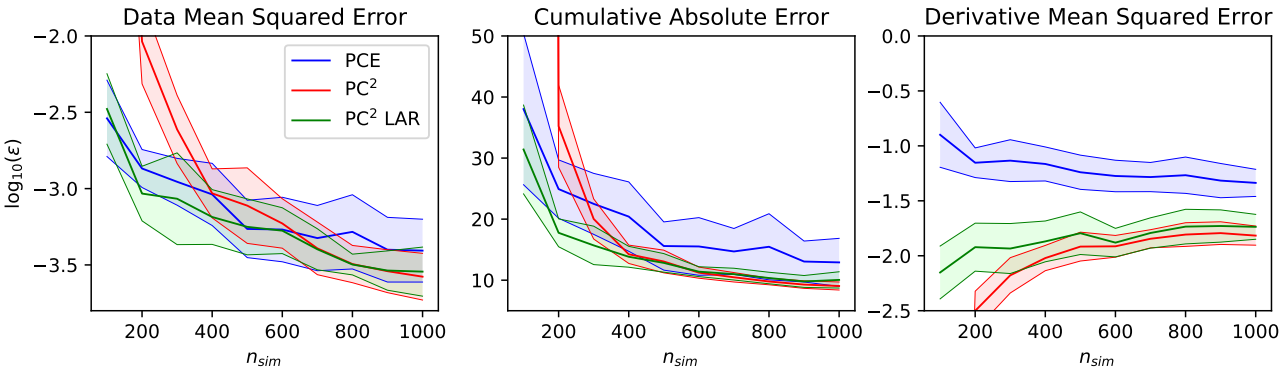

Figure 3: Numerical results for the 3D horseshoe for increasing number of samples in the domain for three different error measures.

Although the underlying IGA model is linear elastic, the mapping from geometric parameters to stress triaxiality can be highly nonlinear. Consequently, even a linear partial differential equation yields a complex nonlinear response surface in the input space. Therefore, a physics-informed surro-

gate, such as IGA-sensitivity-based PC^2, has great potential for UQ when it comes to accurately and efficiently quantifying geometric uncertainty.

6 CONCLUSIONS

The present paper introduces a novel strategy for geometric uncertainty quantification, whereby variational sensitivities from Isogeometric Analysis (IGA) are integrated into a Physics-informed Polynomial Chaos Expansion (PC^2). The proposed IGA-sensitivity-based PC^2 surrogate was applied to estimate stress triaxiality in a 3D horseshoe geometry with four independent geometric uncertain parameters. The IGA-sensitivity-based PC^2 surrogate demonstrated superior performance in terms of mean squared error, cumulative absolute error, and derivative fidelity metrics when compared to the standard sparse PCE. The integration of IGA-derived constraints through a Karush-Kuhn-Tucker (KKT) formulation has been demonstrated to result in a substantial reduction in the number of required training runs. Furthermore, this approach has been demonstrated to enhance predictive accuracy and accurately capture gradient behavior.

The principal strengths of this approach are twofold. Firstly, IGA's exact geometric representation and efficient variational sensitivity calculation generate high-value training information at negligible extra cost. Secondly, the KKT-based enforcement of physics guarantees that both data and governing equations are satisfied in the surrogate. Consequently, the combination of these characteristics renders IGA-sensitivity-based PC^2 particularly well-suited for the execution of computationally intensive IGA-based UQ in complex systems.

Nevertheless, there are several potential areas for further refinement. The present implementation is based on the assumption of linear elasticity and static systems. Extensions to nonlinear material behaviour, coupled dynamics, or correlated input parameters will require careful adaptation of both sensitivity extraction and constraint enforcement. Furthermore, while the horseshoe example is representative of many engineering components, real-world applications may involve higher-dimensional design spaces or localized geometric discontinuities, which could pose a challenge to the conditioning of the KKT system. Future work will explore applying this method to more complex systems, robust strategies for handling nonlinear and coupled PDEs within the IGA-sensitivity-based PC^2 and investigating its potential for other types of uncertainty.

REFERENCES

[1] Kim, J. and Lee, I. Modeling of geometric uncertainties in topology optimization via the shift of design nodes. *Structural and Multidisciplinary Optimization* (2022). **65**(7).

[2] Zienkiewicz, O.C. and Taylor, R.L. *The finite element method*. McGraw Hill, Vol. I., (1989), Vol. II., (1991).

[3] Hughes, T.J.R. and Cottrell, J.A. and Bazilevs, Y. Isogeometric analysis: CAD, finite elements, NURBS, exact geometry and mesh refinement. *Computer Methods in Applied Mechanics and Engineering* (2005). **194**(39–41):4135–4195.

[4] Wiener, N. The Homogeneous Chaos. *American Journal of Mathematics* (1938). **60**(4):897–936.

[5] Blatman, G. and Sudret, B. Adaptive sparse polynomial chaos expansion based on least angle regression. *Journal of Computational Physics* (2011). **230**(6):2345–2367.

[6] Novák, L., Sharma, H. and Shields, M.D. Physics-informed polynomial chaos expansions. *Journal of Computational Physics* (2024). **506**:112926.

[7] Ghanem, R. and Brzakala, W. Stochastic Finite-Element Analysis of Soil Layers with Random Interface. *Journal of Engineering Mechanics* (1996). **122**(4):361–369.

[8] Nouy, A., Chevreuil, M. and Safatly, E. Fictitious domain method and separated representations for the solution of boundary value problems on uncertain parameterized domains. *Computer Methods in Applied Mechanics and Engineering* (2011). **200**(45–46):3066–3082.

[9] Zheng, Z., Valdebenito, M., Beer, M. and Nackenhorst, U. A stochastic finite element scheme for solving partial differential equations defined on random domains. *Computer Methods in Applied Mechanics and Engineering* (2023). **405**:115860.

[10] Zhang, H. and Shibutani, T. Development of stochastic isogeometric analysis (SIGA) method for uncertainty in shape. *International Journal for Numerical Methods in Engineering* (2018). **118**(1):18–37.

[11] Lüthen, N., Roustant, O., Gamboa, F., Iooss, B., Marelli, S., Sudret, B. Global sensitivity analysis using derivative-based sparse Poincaré chaos expansions. *International Journal for Uncertainty Quantification* (2023). **13**:57–82.

[12] Sudret, B. Global sensitivity analysis using polynomial chaos expansions. *Reliability Engineering & System Safety* (2008). **93**(7):964–979.

[13] Sharma, H., Novák, L. and Shields, M. Physics-constrained polynomial chaos expansion for scientific machine learning and uncertainty quantification. *Computer Methods in Applied Mechanics and Engineering* (2024). **431**:117314.

[14] Olivier, A., Giovanis, D., Aakash, B., Chauhan, M., Vandanapu, L. and Shields, M.D. UQpy: A general purpose Python package and development environment for uncertainty quantification. *Journal of Computational Science* (2020). **47**:101204.

[15] Cottrell, J.A. *Isogeometric analysis: Toward integration of CAD and FEA*. Edited by Hughes, T.J.R. and Bazilevs, Y. Wiley, Chichester, West Sussex, U.K., (2009).

[16] de Boor, C. Subroutine package for calculating with B-splines. *Technical Report LA-4728-MS, Los Alamos Scientific Laboratory, Los Alamos, NM*, (1971), pp. 109, 121.

[17] Liedmann, J. and Barthold, F.-J. Variational sensitivity analysis of elastoplastic structures applied to optimal shape of specimens. *Structural and Multidisciplinary Optimization* (2020). **61**(6):2237–2251.

[18] Spink D.M. NURBS Toolbox. *MATLAB Central File Exchange* (2020). Retrieved December 14, 2020.

[19] Manque, N.A., Liedmann, J., Barthold, F.-J., Valdebenito, M.A. and Faes, M.G.R. Interval Isogeometric Analysis for coping with geometric uncertainty. *Computer Methods in Applied Mechanics and Engineering* (2025). **437**:117773.